

University of Groningen

Identification of novel peroxisome functions in yeast

Singh, Ritika

DOI:
[10.33612/diss.99106402](https://doi.org/10.33612/diss.99106402)

IMPORTANT NOTE: You are advised to consult the publisher's version (publisher's PDF) if you wish to cite from it. Please check the document version below.

Document Version
Publisher's PDF, also known as Version of record

Publication date:
2019

[Link to publication in University of Groningen/UMCG research database](#)

Citation for published version (APA):
Singh, R. (2019). *Identification of novel peroxisome functions in yeast*. [Thesis fully internal (DIV), University of Groningen]. University of Groningen. <https://doi.org/10.33612/diss.99106402>

Copyright

Other than for strictly personal use, it is not permitted to download or to forward/distribute the text or part of it without the consent of the author(s) and/or copyright holder(s), unless the work is under an open content license (like Creative Commons).

The publication may also be distributed here under the terms of Article 25fa of the Dutch Copyright Act, indicated by the "Taverne" license. More information can be found on the University of Groningen website: <https://www.rug.nl/library/open-access/self-archiving-pure/taverne-amendment>.

Take-down policy

If you believe that this document breaches copyright please contact us providing details, and we will remove access to the work immediately and investigate your claim.

Downloaded from the University of Groningen/UMCG research database (Pure): <http://www.rug.nl/research/portal>. For technical reasons the number of authors shown on this cover page is limited to 10 maximum.

CHAPTER

3

Stress exposure results in increased peroxisomal levels of yeast Pnc1 and Gpd1, which are imported via a piggy-backing mechanism

Ritika Singh¹, Sanjeev Kumar¹,
Chris P. Williams and Ida J. van der Klei^{*}

Molecular Cell Biology, Groningen Biomolecular Sciences and Biotechnology
Institute (GBB), University of Groningen, P.O. Box 11103, 9700CC
Groningen, The Netherlands

¹These authors equally contributed to this paper

Abstract

3

Saccharomyces cerevisiae glycerol phosphate dehydrogenase 1 (Gpd1) and nicotinamidase (Pnc1) are two stress- induced enzymes. Both enzymes are predominantly localised to peroxisomes at normal growth conditions, but were reported to localise to the cytosol and nucleus upon exposure of cells to stress. Import of both proteins into peroxisomes depends on the peroxisomal targeting signal 2 (PTS2) receptor Pex7. Gpd1 contains a PTS2, however, Pnc1 lacks this sequence.

Here we show that Pnc1 physically interacts with Gpd1, which is required for piggy-back import of Pnc1 into per- oxisomes. Quantitative fluorescence microscopy analyses revealed that the levels of both proteins increased in peroxisomes and in the cytosol upon exposure of cells to stress. However, upon exposure of cells to stress we also observed enhanced cytosolic levels of the control PTS2 protein thiolase, when produced under control of the GPD1 promoter. This suggests that these conditions cause a partial defect in PTS2 protein import, probably because the PTS2 import pathway is easily saturated.

Introduction

Saccharomyces cerevisiae Gpd1 (Glycerol-3-phosphate dehydrogenase 1) and Pnc1 (nicotinamidase) are peroxisomal enzymes that are induced upon exposure of cells to various stress conditions¹⁻⁴. Gpd1 is a nicotinamide adenine dinucleotide-hydrogen (NADH)-dependent enzyme that converts dihydroxyacetone phosphate (DHAP) into glycerol-3-phosphate, which subsequently can be converted into glycerol⁵. At osmotic stress conditions Gpd1 activity increases, which leads to enhanced cellular glycerol levels and osmotic stress resistance⁶. At normal conditions, Gpd1 contributes to reducing cellular DHAP levels, which prevents the spontaneous conversion of DHAP into methylglyoxal, a highly toxic compound that damages proteins and contributes to ageing^{7,8}. In addition, Gpd1 may play a role in controlling the redox balance by reoxidation of NADH to NAD⁺. Pnc1 functions in the NAD⁺ salvage pathway and catalyses deamination of nicotinamide to nicotinic acid⁹. Overexpression of Pnc1 has been reported to positively affect the replicative lifespan of yeast¹. It has been suggested that this is the result of Pnc1-mediated nicotinamide depletion in the nucleus, which activates the histone deacetylase Sir2, resulting in silencing of pro-ageing genes^{1,10}. Pnc1 levels are elevated under conditions known to extend replicative lifespan, including osmotic and heat stress, conditions that also enhance Gpd1 levels¹. Interestingly, examination of transcriptional profiles revealed that PNC1 expression is strongly correlated with that of GPD1¹¹.

Although the above functions of Gpd1 and Pnc1 are expected to take place in the cytosol and nucleus respectively, at normal growth conditions both enzymes are predominantly localised to peroxisomes in conjunction with a minor portion to the cytosol^{1,11}. When Gpd1 and Pnc1 levels were enhanced upon exposure of cells to osmotic stress, a much higher portion of these enzymes became cytosolic concomitant with a relative decrease in the peroxisomal protein levels¹¹. However, it has also been reported that Pnc1 mainly remains peroxisomal in cells exposed to stress¹.

The peroxisomal localisation of Gpd1 depends on its N-terminal peroxisomal targeting signal 2 (PTS2) and the PTS2-receptor Pex7¹¹. It has been suggested that import of Gpd1 into peroxisomes is stimulated by the phosphorylation of two serine residues adjacent to the PTS2 sequence. The enhanced cytosolic Gpd1 level in cells exposed to stress was proposed to be due to decreased phosphorylation of these residues^{11,12}.

Sequence analysis did not reveal any predicted peroxisomal targeting signals in Pnc1. However, sorting of Pnc1 requires the PTS2 import machinery, because the protein mislocalises to the cytosol in $\Delta pex7$ cells¹. Computational analysis revealed that Pnc1 may form a complex with¹³. If so, Pnc1 may import into peroxisomes in complex with Gpd1 by so called piggy-back import.

Here we show that Pnc1 and Gpd1 proteins indeed physically interact in vivo and that this allows piggy-back import of Pnc1 with Gpd1. Furthermore, quantitative fluorescence microscopy analysis revealed that upon exposure of the cells to osmotic stress the peroxisomal as well as the cytosolic levels of both proteins increased. Our data indicate that the appearance of cytosolic Gpd1 and Pnc1 most likely is caused by a general decrease in the rate of PTS2-

matrix protein import in yeast cells exposed to stress, probably because this pathway is easily saturated.

Results

3

Pnc1 is targeted to peroxisomes via piggy-back import with Gpd1

Piggy-back import requires that Pnc1 and Gpd1 physically interact in vivo. To test this we performed yeast two-hybrid analysis. As shown in Fig. 1, activation of the reporter gene HIS3, indicated by the capacity of yeast transformants to grow in the absence of histidine, was observed when PNC1 was co-expressed with GPD1. Similarly, growth was observed in strains co-expressing *H. polymorpha* PEX3 and PEX19, which were used as positive controls. Growth was not observed in control experiments using empty plasmids or in strains expressing either GPD1 or PNC1.

Next, we tested whether the peroxisomal localisation of Pnc1 depends on Gpd1. As shown in Fig. 2A, B, in cells producing chromosomally tagged GFP-fusion proteins, Gpd1-GFP and Pnc1-GFP are predominantly co-localising with the peroxisomal marker protein DsRed-SKL, in conjunction with low fluorescence in the cytosol. Accumulation of the proteins in the nucleus was not observed. The peroxisomal localisation of Pnc1-GFP was fully abolished in Δ gpd1 cells (Fig. 2C). Conversely, in Δ pnc1 cells the peroxisomal localisation of Gpd1-GFP was unaffected (Fig. 2D). This result indicates that import of Pnc1 depends on the presence of Gpd1, consistent with piggy-back import.

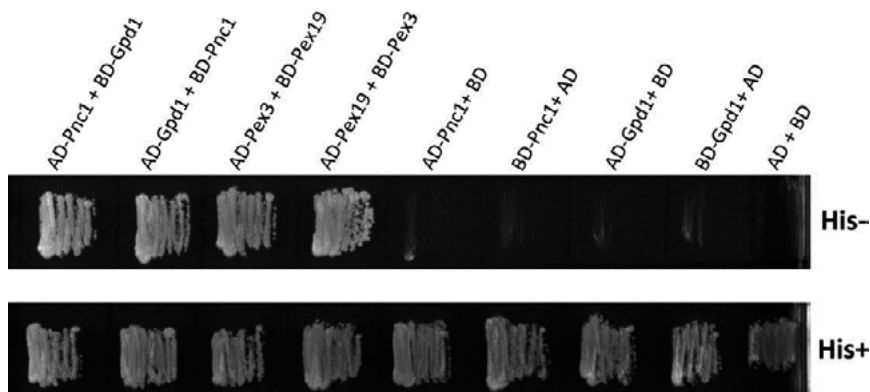


Figure 1. In vivo interaction of Gpd1 and Pnc1. Full length Gpd1 and Pnc1 were tested for interaction using a yeast two-hybrid assay. Genes were fused to the LEXA binding domain (BD) in vector pBTM116-C and a VP16 activation domain (AD) in vector pVP16-C. The resulting plasmids were co-transformed into *S. cerevisiae* L-40. The interaction between *H. polymorpha* Pex3 and Pex19 is used as positive control [18]. As negative controls, empty pVP16-C or pBTM116-C was used. HIS3 reporter gene activation was detected by analysis of growth on plates lacking histidine.

Next, we tested the effect of the removal of the PTS2 from the N-terminus of Gpd1 on the localisation of NΔGpd1-mCherry and Pnc1-GFP fusion proteins. As shown in Fig. 2E in cells producing the N-terminal truncated Gpd1 the peroxisomal localisation of both proteins was abolished.

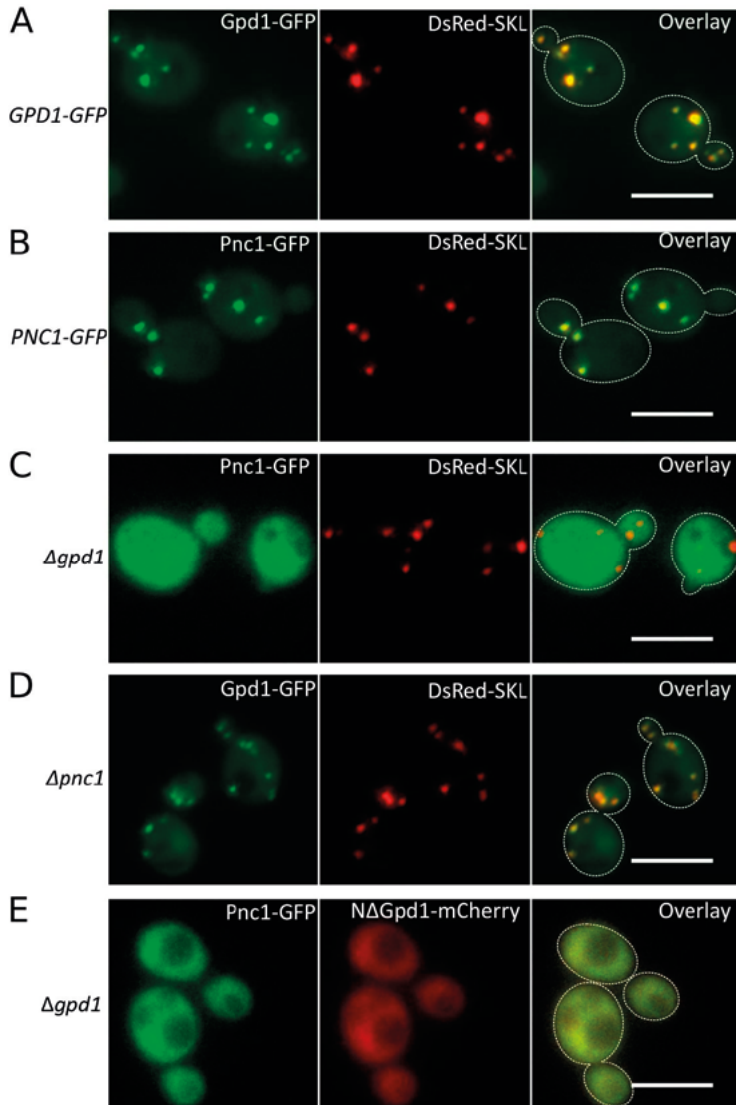


Figure 2. The peroxisomal localisation of Pnc1 depends on Gpd1. Fluorescence microscopy images showing the localisation of chromosomally tagged Gpd1-GFP (A) and Pnc1-GFP (B) in *S. cerevisiae* cells producing DsRed-SKL as red peroxisomal matrix marker. Localisation of Pnc1-GFP in $\Delta gpd1$ cells (C) or Gpd1-GFP in $\Delta pnc1$ cells (D) both producing DsRed-SKL as peroxisomal marker. (E) $\Delta gpd1$ cells producing Pnc1-GFP and NΔGpd1-mCherry. The bar represents 5 μm .

We also investigated whether we could restore import of NΔGpd1-mCherry into peroxisomes by the addition of a C-terminal PTS1 to Pnc1 (Pnc1-SKL). In Δgpd1 cells all NΔGpd1-mCherry was cytosolic (Fig. 3A; compare Fig. 2E). However, upon co-production of Pnc1-SKL a portion of the NΔGpd1-mCherry protein localised to peroxisomes (Fig. 3B). The import of only a minor portion of the total NΔGpd1-mCherry is most likely related to the fact that Gpd1 is present in large excess relative to Pnc1 (see below).

Taken together, these results strongly suggest that Pnc1 is imported into peroxisomes via piggy-backing with Gpd1.

Pnc1 and Gpd1 stability

If both proteins form a stable complex *in vivo*, the absence of one component of the complex might cause instability of the other proteins and vice versa. To test this we analysed the levels of Pnc1-GFP in Δgpd1 cells and vice versa in cells in the stationary ($T = 0$), early exponential ($T = 4$), mid-exponential ($T = 8$ h) and late-exponential ($T = 12$ h) growth phase. The levels of Pnc1-GFP are comparable in Δgpd1 cells relative to the wild-type (PNC1-GFP) control strain (Fig. 4A). Similarly, the levels of Gpd1-GFP are not reduced in Δpnc1 cells (Fig. 4B). These results imply that Pnc1 and Gpd1 are not required for the stability of each other. In the absence of Gpd1, Pnc1 localises to the cytosol. As no major difference in Pnc1 levels is observed between wild-type and Δgpd1 cells the peroxisomal versus cytosolic localisation apparently also does not affect Pnc1 stability.

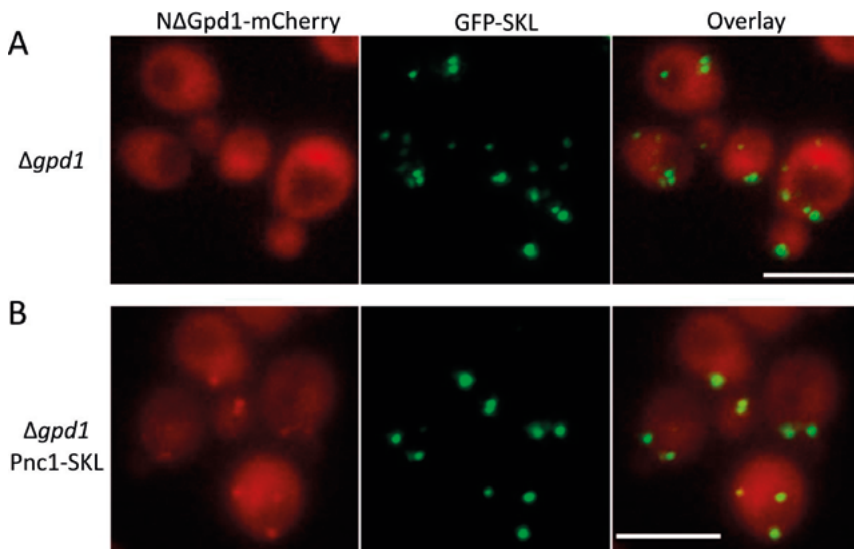


Figure 3. Import of Gpd1 lacking a PTS2 is restored by co-production with Pnc1 containing a PTS1 signal. Localisation of NΔGpd1-mCherry in Δgpd1 cells (A) or in Δgpd1 cells producing Pnc1-SKL. The PTS1 (-SKL) is chromosomally added to endogenous PNC1. (B). Peroxisomes are marked with GFP-SKL. The scale bar represents 5 μm.

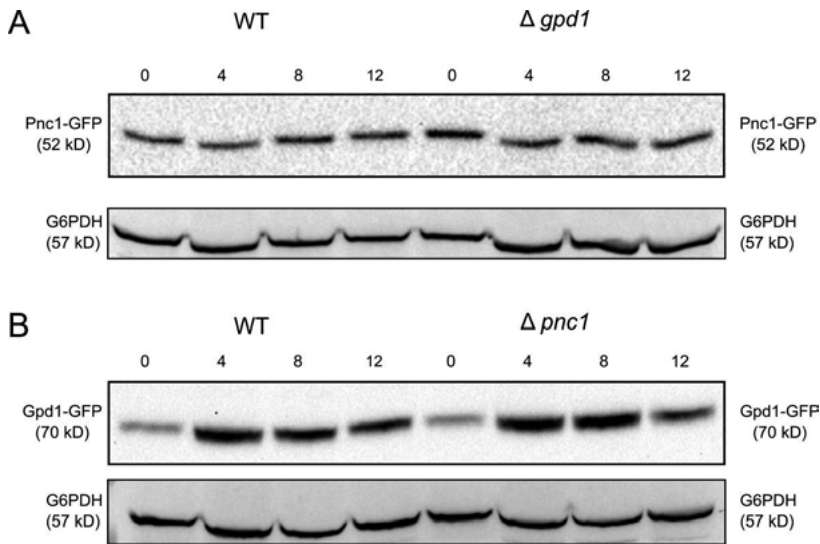


Figure 4. Fig. 4. Gpd1 and Pnc1 do not stabilise each other. Stationary glucose cultures (0 h) were diluted into fresh glucose medium and grown for 4, 8 or 12 h. Cellular protein levels of Pnc1-GFP (A) and Gpd1-GFP (B) were analysed in $\Delta gpd1$ (A) and $\Delta pnc1$ cells (B) using WT cells as controls. Blots were probed with antibodies against GFP. Glucose-6-phosphate dehydrogenase (G6PDH) was used as loading control.

Gpd1 and Pnc1 are not present at a fixed stoichiometry

Previous transcriptional analysis indicated that GPD1 and PNC1 expression is strongly correlated¹¹. In order to analyse whether the protein levels of Gpd1 and Pnc1 are correlated as well, we performed Western blot analysis using strains producing GFP fusion proteins and anti-GFP antibodies. Upon exposure of cells for 4 h to 1 M sorbitol, 1 M NaCl or elevated temperature (37 °C), the levels of both proteins were enhanced (Fig. 5A). Quantification of the protein levels revealed that the ratio between Gpd1 and Pnc1 was approximately 7:1 in un-stressed control cells, but increased considerably in cells exposed to stress (up to ~ 11:1 upon exposure to 1 M NaCl) (Fig. 5B). This result indicates that both proteins most likely do not form a hetero-oligomeric complex of fixed stoichiometry. Notably, at all conditions analysed, Gpd1 was present in large excess relative to Pnc1.

Gpd1 and Pnc1 are localised to peroxisomes and the cytosol in cells exposed to stress

Jung and colleagues reported that exposure of cells to stress results in a decrease in peroxisomal Gpd1 and Pnc1 levels concomitant with a relative increase in cytosolic protein levels¹¹. In contrast, Anderson and colleagues showed that Pnc1 mainly remains peroxisomal in cells exposed to stress¹.

We performed quantitative fluorescence microscopy to analyse the mean cytosolic and peroxisomal fluorescence intensities of Gpd1-GFP (Fig. 5D) and Pnc1-GFP (Fig. 5C) before

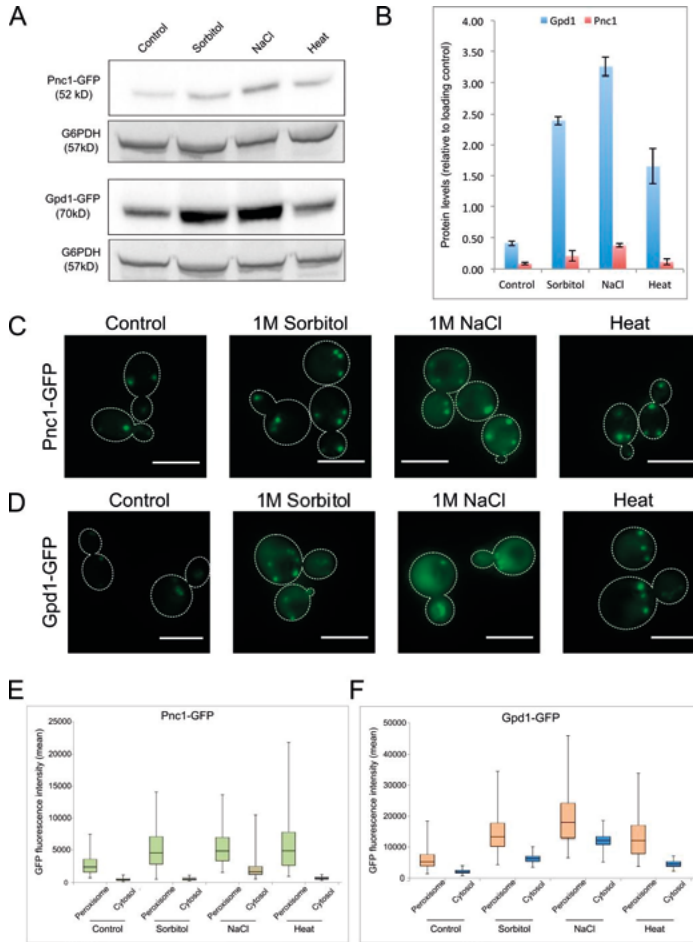


Figure 5. Modulations in Gpd1 and Pnc1 protein levels and localisation upon exposure of cells to stress. (A) Western blots showing the protein levels of Pnc1-GFP and Gpd1-GFP after exposure to various stress conditions for 4 h. Cells producing chromosomally tagged GFP-fusion proteins under control of their endogenous promoter were used for the experiments. Blots were probed with antibodies against GFP. G6PDH was used as loading control. (B) Quantification of Gpd1-GFP and Pnc1-GFP protein levels from 2 separate blots of 2 independent experiments. Error bar = \pm STDV. Fluorescence microscopy images of Pnc1-GFP (C) and Gpd1-GFP (D) cells at control conditions (unstressed) or upon exposure to stress for 4 h. The scale bar represents 5 μ m. The box plot shows mean fluorescence intensities of Pnc1-GFP (E) and Gpd1-GFP (F) at peroxisomes or in the cytosol after 4 h of stress. Fluorescence intensities were measured using ImageJ. The box represents values from the 25 percentile to the 75 percentile; the horizontal line through the box represents the median value. The bar represents maximum and minimum values. For each experiment the fluorescence intensity of at least 100 peroxisomes and the cytosol of at least 44 cells were measured.

and after exposure of cells to various stress conditions. Because we rarely observed significant accumulation of Gpd1 or Pnc1 in the nucleus at our experimental set up, we excluded nuclear GFP signal in our analysis.

Our data indicate that at all three stress conditions tested (1 M sorbitol, 1 M NaCl, heat stress) the fluorescence intensities of peroxisomal Pnc1–GFP and Gpd1–GFP increased relative to the controls (Fig. 5E, F; Table 1). All three stress conditions also resulted in an increase in cytosolic Gpd1–GFP, whereas enhanced cytosolic Pnc1–GFP was only detected upon exposure of cells to 1 M NaCl.

To test whether this behaviour is specific for Gpd1 and Pnc1, we performed a control experiment in which we produced the PTS2 protein Pot1 (thiolase) containing a C-terminal GFP under control of the GPD1 promoter. Western blot analysis of GFP fusion proteins using anti-GFP antibodies revealed that similar protein levels were obtained for Pot1–GFP and Gpd1–GFP upon exposure of cells to osmotic stress (Fig. 6A).

Quantitative fluorescence microscopy (images shown in Fig. 6B, C & D) indicated that similar to Gpd1–GFP the fluorescence intensity of Pot1–GFP also increased in both the cytosol and peroxisomes after treatment of cells with 1 M sorbitol or 1 M NaCl (Fig. 6E, F).

These results indicate that import of Gpd1 and Pnc1 is not blocked upon exposure of cells to stress. However, our data suggest that the capacity of the PTS2 import machinery is inefficient to fully import the enhanced levels of Gpd1 and Pnc1 at these conditions.

Conclusions

In this paper we show that yeast Pnc1 piggy-back imports with Gpd1 into peroxisomes. Almost all peroxisomal matrix proteins contain either a PTS1 or PTS2 sorting sequence. However, proteins lacking a PTS can be imported in complex with a PTS containing protein by so called piggy-back import. Many reported examples of peroxisomal piggy-back import are artificial as these involve import of a subunit of an oligomeric protein from which the PTS is removed in complex with subunits that still contain a PTS^{14–16}. So far only a few examples of natural piggy-back import have been described. These include import of the PTS lacking Cu/Zn superoxide dismutase 1 (SOD1) with its PTS-containing chaperone in mammalian cells¹⁷. In plant, import of two PTS lacking subunits of heterotrimeric protein phosphatase

Table 1. Fold increase in median fluorescence intensities of Gpd1–GFP and Pnc1–GFP in cells exposed to stress relative to control cells.

	Gpd1–GFP		Pnc1–GFP	
	Peroxisomes	Cytosol	Peroxisomes	Cytosol
Control	1.0	1.0	1.0	1.0
Sorbitol	2.6	3.0	1.9	1.2
NaCl	3.5	5.8	2.1	3.3
Heat	2.3	2.2	2.1	1.3

depends on the PTS containing third subunit of this enzyme¹⁸. Here, we report natural piggy-back import of Pnc1 with the PTS2 protein Gpd1 into yeast peroxisomes. Effelsberg et al.¹⁹ recently reported the same observation. In addition, these authors showed that import of Gpd1 requires the general Pex7 co-receptor Pex21, a protein that is constitutively produced. Instead the second Pex7 co-receptor Pex18 is induced by oleate and selectively required for import of the β -oxidation enzyme thiolase.

Why Pnc1 piggy-back imports with Gpd1 and not with another PTS2 or PTS1 protein is highly speculative. Possibly this is related to the fact that Gpd1 and Pnc1 are both involved in stress response and nucleotide metabolism. Also their expression is regulated in a similar manner.

Although we observed that Pnc1 and Gpd1 interact in a two-hybrid assay, Pnc1 and Gpd1 most likely do not form a stable complex. This view is based on the finding that i) the absence of one protein did not affect the stability of the other and ii) the cellular ratio of both proteins is not constant. Also, we were unable to show a stable physical interaction between both proteins using a variety of in vitro approaches (data not shown). These observations imply that complex formation between Gpd1 and Pnc1 likely is transient and possibly only required for sorting of Pnc1 to peroxisomes.

Our data confirm earlier reports which indicated that upon exposure of yeast cells to stress conditions the protein levels of Gpd1 and Pnc1 increase. Our quantitative fluorescence microscopy analyses showed that under these conditions the intensities of Gpd1-GFP and Pnc1-GFP inside peroxisomes increased. This increased peroxisomal signal is in contrast with previous observations of Jung and colleagues, who reported a decrease in peroxisomal signal for both proteins¹¹. However, our data are in line with the report of Anderson and colleagues, who showed that Pnc1-GFP remains predominantly peroxisomal upon exposure of cells to stress.

At all stress conditions tested we observed an increase in cytosolic fluorescence intensities of Gpd1-GFP, but not of Pnc1-GFP, for which an increase in cytosolic fluorescence was only detected upon exposure of cells to NaCl. This could be due to the higher total Gpd1 protein levels upon exposure of cells to stress (see Western blots in Fig. 5A). Also the ratio of Gpd1-Pnc1 increased at stress conditions, thus rendering more Gpd1 molecules available to Pnc1 for piggy-back import.

When a control PTS2 protein (thiolase, Pot1-GFP) was produced under control of the GPD1 promoter, we also observed the appearance of cytosolic fluorescence when cells were exposed to stress. This result suggests that PTS2 protein import is inefficient in cells exposed to stress, probably because the PTS2 import pathway is easily saturated.

Consequently, both proteins most likely play their cellular function inside peroxisomes and not in the cytosol or nucleus as previously proposed. What their function is in peroxisomes is still very speculative. Peroxisomes are highly oxidative organelle and therefore maintenance of a proper redox environment is crucial for functioning of peroxisomal enzymes. Because both proteins are involved in nucleotide metabolism, possibly they play a role in maintaining the redox balance in the peroxisomal matrix.

Materials and methods

Strains and growth conditions

The *S. cerevisiae* strains used in this study are listed in Supplementary Table 1. Yeast cells were grown at 30 °C on mineral medium (MM)²⁰ containing 0.25% ammonium sulphate and 2% glucose. MM was supplemented with the required amino acids or uracil to a final concentration of 20 µg ml⁻¹ (histidine and methionine) or 30 µg ml⁻¹ (leucine, lysine, and uracil). YPD medium (1% yeast extract, 1% peptone, 1% glucose) supplemented with 2% agar was used for growth on plates. *Escherichia coli* DH5α was used for cloning purposes and was cultured at 37 °C on LB medium supplemented with the appropriate antibiotics.

Construction of yeast strains

Plasmids and primers used in this study are listed in Supplementary Tables 2 and 3 respectively.

Construction of Δpnc1 and Δgpd1 strains

GPD1 was deleted in a strain producing Pnc1–GFP obtained from GFP fusion collection²¹, by replacing the ORF with the KanMX4 gene from pUG6²² using primers GPD1F and GPD1R. Pnc1–GFP producing cells were transformed with the PCR product, colonies were selected on YPD plates containing 200 µg ml⁻¹ G418, and positive clones were checked by colony PCR. Correct integration was confirmed by Southern blotting. PNC1 deletion in Gpd1–GFP producing cells obtained from GFP fusion collection²¹ was obtained by replacement of the ORF with the KanMX4 gene from pUG6 using primers PNC1F and PNC1R. Cells were transformed with the PCR product and transformants were selected on YPD plates containing 200 µg ml⁻¹ G418, positive clones were checked by colony PCR and Southern blot.

Strains producing NΔGpd1 and NΔGpd1–mCherry

To construct a strain lacking 17 N-terminal amino acid residues (+ 4 to + 54 bps) of Gpd1 after the start codon, a plasmid pAG25- N_del_Gpd1 was cloned and transformed into Δgpd1 strain obtained from Euroscarf. To this end, the GPD1 coding region + 55 (+ 1 is A of the start codon) from the start codon (without PTS2 sequence) and the GPD1 promoter region – 540 from the start codon were amplified from *S. cerevisiae* genomic DNA using the primer pairs GPD1.OL-1/GPD1.OL-1.1 and GPD1.OL-2/GPD1.OL-2.1 respectively.

The two PCR products of 1457 bps and 472 bps were joined together by overlap PCR and the combined fragment was further amplified using primer pair GPD1.OL-1.1/GPD1.OL-2.1, which resulted into a fragment of 1984 bps. This fragment was digested with HindIII/BamHI and cloned in plasmid pAG25²³ resulting in plasmid pAG25-N_del_Gpd1. The insert was sequenced to exclude the presence of errors. The plasmid was linearised with SbfI and transformed to *S. cerevisiae* Δgpd1 cells. Transformants were selected on YPD plates containing 100 µg ml⁻¹ nourseothricin (WERNER BioAgents). Correct integration in the genomic DNA was checked by colony PCR and Southern blotting. The resulting strain that produces NΔGpd1 but not the endogenous Gpd1 was designated as nΔgpd1.

To introduce mCherry at the C-terminus of NΔGPD1, the mCherry–zeocin fragment was amplified from pHIPZ4–mCherry usinator plasmid using primer pair GPD1.MC_F/GPD1.MC_R2. The PCR product was used to transform *S. cerevisiae* competent cells and plated on YPD plates containing 200 μg ml⁻¹ zeocin (Invitrogen). Positive clones were checked by colony PCR.

Construction of a strain producing NΔGpd1–mCherry and Pnc1–SKL

To obtain a plasmid containing the zeocin resistance gene and a gene encoding Pnc1–SKL, PNC1 genomic DNA starting from –700 was amplified using primers P.SKL.F_BamHI and P.SKL.R_HindIII. The PCR product was digested with BamHI/HindIII and cloned into pSL34 resulting in pPNC1–SKL-1. To add the PTS1 tripeptide –SKL to endogenous Pnc1, the region encoding the 3'-end of the PNC1 gene along with the –SKL (PTS1) coding region and the zeocin resistance gene were amplified from pPNC1–SKL-1 using primers PNC1.7 and PNC1.GFP.SKL-2.2. The PCR product was used to transform nΔgpd1 cells and clones were selected on YPD/zeocin plates. mCherry was introduced at the C-terminus of NΔGpd1 in the resulting strain as follows: the mCherry–hph (Hygromycin R) fragment was amplified from pARM001 (see below) using primer pair GPD.MC_F/GPD1.MC_Rev. The PCR product was used to transform nΔgpd1.PNC1–SKL competent cells and transformants were selected on YPD plates with 200 μg ml⁻¹ hygromycin. Positive clones were checked by colony PCR. The resulting strain produces Pnc1–SKL and NΔGpd1–mCherry but not endogenous Gpd1.

Construction of a strain producing Pot1–GFP under control of the GPD1 promoter

The GPD1 promoter starting from –700 bps of the start codon and the POT1 open reading frame were amplified from *S. cerevisiae* genomic DNA using primer pairs P-GPD1.PciI/GPD1.OL-Rev. and POT1.OL-Fw/POT1-BglII that resulted in PCR products of 731 bps and 1284 bps, respectively. Both DNA fragments were joined together by overlap PCR and combined fragment was further amplified using primer pair P-GPD1.PciI/POT1-BglII, which resulted in a DNA fragment of 1973 bps. The combined fragment was digested by restriction enzymes NciI/BglII and cloned into the pHIPZ–mGFP usinator plasmid²⁴ which resulted in pPGPD1–POT1–GFP. The plasmid was linearised by SbfI and transformed into *S. cerevisiae* strain producing DsRed1–SKL. Transformants were selected on YPD/zeocin plates and checked by colony PCR.

Construction of other plasmids

Construction of pSL33. To construct a plasmid producing DsRed–SKL under control of the MET25 promoter, the PMET25–DsRed–SKL–tcyc1 fragment was amplified from pUG34–DsRed–SKL²⁵ using primer pair DsRed-1/DsRed-2. The obtained PCR product was digested with KpnI/XbaI and cloned into pBSII KS + resulting in pSL32. The nourseothricin resistance gene was amplified from pAG25 using primer pair Nat1.1/Nat1.2 and after digestion with SacII/KpnI the fragment was cloned into pSL32 that resulted in pSL33.

Construction of pPTDH3–GFP–SKL

The promoter of the TDH3 gene was amplified from *S. cerevisiae* genomic DNA by using primer pair TDH3_Not.F/TDH3_BamHI.R. A fragment of 716 bps was obtained that was digested with NotI/BamHI and cloned into pHIPX7–GFP–SKL²⁶ resulting in pPTDH3–GFP–SKL. To mark peroxisomes with GFP–SKL, the plasmid was linearised with BseYI and used to transform *S. cerevisiae* strains, and transformants were selected on YND plates without leucine. Correct integration was checked by colony PCR.

Construction of pARM001

The PEX14–mCherry region of pHIPN– PEX14–mCherry²⁰ was amplified using primer pair PRARM001 FWD/PRARM002 REV. The PCR product was digested with NotI/HindIII and clone into pHIPH4²⁷ that resulted into pARM001.

Construction of pHIPZ4–mCherry fusinator

For the construction of plasmid pHIPZ4–mCherry fusinator, a PCR fragment of 700 bp was obtained by primer pair RSA10fw/RSA11rev on pCDNA3.1mCherry²⁸. The resulting BglII–SalI fragment was inserted between the BglII and SalI of pANL31²⁹.

Yeast two-hybrid assays

The LexA system was used for screening interactions between *S. cerevisiae* proteins using derivatives of the reporter strain *S. cerevisiae* L-40 (Takara Bio Inc.). Using *S. cerevisiae* genomic DNA as template, the entire coding sequences of PNC1 and GPD1 were amplified with primer combinations PNC1.BamHI.F/PNC1.EcoRI.R and GPD1.BamHI.F/ GPD1.EcoRI.R, respectively. The PCR fragments were digested with BamHI/EcoRI and separately cloned into the vectors pBTM116–C and pVP16–C, which yielded plasmids pBTM116–PNC1, pVP16– PNC1, pBTM116–GPD1 and pVP16–GPD1. *S. cerevisiae* L-40 was co- transformed with the indicated pVP16- and pBTM116-derived fusion constructs and transformants were selected on synthetic medium lacking leucine and tryptophan. HIS3 reporter gene activation was detected by analysing growth on medium lacking histidine, leucine and 3-aminotriazole. From each co-transformation four independent transformants were tested. Empty vectors were used to check for reporter self-activation. The well-established *Hansenula polymorpha* Pex3 *H. polymorpha* Pex19 interaction²⁴ was used as a positive control.

Western blotting

Proteins of total cell extracts of²⁶ trichloroacetic acid treated cells were separated by SDS-PAGE followed by Western blotting. Equal amounts of protein were loaded per lane. Blots were probed with mouse monoclonal antiserum against GFP (Santa Cruz Biotechnology, sc-9996) and rabbit polyclonal antiserum against glucose-6-phosphate dehydrogenase (G6PD), which was used as a loading control. Secondary antibodies conjugated to horseradish peroxidase were used for detection. Blots were scanned using a densitometer (Biorad).

Fluorescence microscopy

All fluorescence images were acquired using a 100×1.30 NA Plan-Neofluar objective (Carl Zeiss). Wide-field microscopy images were captured by an inverted microscope (Observer Z1; Carl Zeiss) using AxioVision software (Carl Zeiss) and a digital camera (CoolSNAP HQ2; Photometrics). GFP signal was visualised with a 470/40-nm band pass excitation filter, a 495-nm dichromatic mirror, and a 525/50-nm band pass emission filter. To visualise DsRed fluorescence, a 546/12-nm bandpass excitation filter, a 560-nm dichromatic mirror, and a 575–640-nm bandpass emission filter were used. mCherry fluorescence was visualised with a 587/25-nm band pass excitation filter, a 605-nm dichromatic mirror, and a 647/70-nm band-pass emission filter.

To analyse the acquired fluorescence images ImageJ software (US National Institutes of Health, Bethesda, MD, USA) was used. For quantification, a straight line was drawn using ImageJ's "line tool" through the region of interest and pixel intensity along the line was measured. The measured mean fluorescence intensity of GFP on peroxisomes and in the cytosol was corrected for the background intensity and a box plot was made using Microsoft Excel.

Acknowledgements

SK is supported by the Netherlands Organization for Scientific Research (NWO) (723.013.004). RK and IvdK are funded by the Marie Curie Initial Training Network PERFUME (PERoxisome Formation, Function, Metabolism) grant (grant agreement number 316723). CW is supported by VIDI grant of NWO.

References

1. Anderson RM, Bitterman KJ, Wood JG, Medvedik O & Sinclair DA (2003) Nicotinamide and PNC1 govern lifespan extension by calorie restriction in *Saccharomyces cerevisiae*. *Nature* **423**, 181–185.
2. Boy-Marcotte E, Lagniel G, Perrot M, Bussereau F, Boudsocq A, Jacquet M & Labarre J (1999) The heat shock response in yeast: differential regulations and contributions of the Msn2p/Msn4p and Hsf1p regulons. *Mol. Microbiol.* **33**, 274–283.
3. Medvedik O, Lamming DW, Kim KD & Sinclair DA (2007) MSN2 and MSN4 link calorie restriction and TOR to sirtuin-mediated lifespan extension in *Saccharomyces cerevisiae*. *PLoS Biol.* **5**, e261.
4. Panadero J, Pallotti C, Rodríguez-Vargas S, Randez-Gil F & Prieto JA (2006) A downshift in temperature activates the high osmolarity glycerol (HOG) pathway, which determines freeze tolerance in *Saccharomyces cerevisiae*. *J. Biol. Chem.* **281**, 4638–4645.
5. Wang HT, Rahaim P, Robbins P & Yocum RR (1994) Cloning, sequence, and disruption of the *Saccharomyces diastaticus* DAR1 gene encoding a glycerol-3-phosphate dehydrogenase. *J. Bacteriol.* **176**, 7091–7095.
6. Albertyn J, Hohmann S, Thevelein JM & Prior BA (1994) GPD1, which encodes glycerol-3-phosphate dehydrogenase, is essential for growth under osmotic stress in *Saccharomyces cerevisiae*, and its expression is regulated by the high-osmolarity glycerol response pathway. *Mol. Cell. Biol.* **14**, 4135–4144.
7. Aguilera J, Rodríguez-Vargas S & Prieto JA (2005) The HOG MAP kinase pathway is required for the induction of methylglyoxal-responsive genes and determines methylglyoxal resistance in *Saccharomyces cerevisiae*. *Mol. Microbiol.* **56**, 228–239.
8. Phillips SA & Thornalley PJ (1993) The formation of methylglyoxal from triose phosphates. Investigation using a specific assay for methylglyoxal. *Eur. J. Biochem.* **212**, 101–105.
9. Ghislain M, Talla E & François JM (2002) Identification and functional analysis of the *Saccharomyces cerevisiae* nicotinamidase gene, PNC1. *Yeast Chichester Engl.* **19**, 215–224.
10. Bitterman KJ, Anderson RM, Cohen HY, Latorre-Esteves M & Sinclair DA (2002) Inhibition of silencing and accelerated aging by nicotinamide, a putative negative regulator of yeast sir2 and human SIRT1. *J. Biol. Chem.* **277**, 45099–45107.
11. Jung S, Marelli M, Rachubinski RA, Goodlett DR & Aitchison JD (2010) Dynamic Changes in the Subcellular Distribution of Gpd1p in Response to Cell Stress. *J. Biol. Chem.* **285**, 6739–6749.
12. Lee YJ, Jeschke GR, Roelants FM, Thorner J & Turk BE (2012) Reciprocal phosphorylation of yeast glycerol-3-phosphate dehydrogenases in adaptation to distinct types of stress. *Mol. Cell. Biol.* **32**, 4705–4717.
13. Qiu J & Noble WS (2008) Predicting co-complexed protein pairs from heterogeneous data. *PLoS Comput. Biol.* **4**, e1000054.
14. Lee MS, Mullen RT & Trelease RN (1997) Oilseed isocitrate lyases lacking their essential type 1 peroxisomal targeting signal are piggybacked to glyoxysomes. *Plant Cell* **9**, 185–197.
15. Glover JR, Andrews DW & Rachubinski RA (1994) *Saccharomyces cerevisiae* peroxisomal thiolase is imported as a dimer. *Proc. Natl. Acad. Sci. U. S. A.* **91**, 10541–10545.
16. Yang X, Purdue PE & Lazarow PB (2001) Eci1p uses a PTS1 to enter peroxisomes: either its own or that of a partner, Dci1p. *Eur. J. Cell Biol.* **80**, 126–138.
17. Islinger M, Li KW, Seitz J, Völkl A & Lüers GH (2009) Hitchhiking of Cu/Zn superoxide dismutase to peroxisomes—evidence for a natural piggyback import mechanism in mammals. *Traffic Cph. Den.* **10**, 1711–1721.
18. Kataya ARA, Heidari B, Hagen L, Kommedal R, Slupphaug G & Lillo C (2015) Protein phosphatase 2A holoenzyme is targeted to peroxisomes by piggybacking and positively affects peroxisomal β -oxidation. *Plant Physiol.* **167**, 493–506.
19. Effelsberg D, Cruz-Zaragoza LD, Tonillo J, Schliebs W & Erdmann R (2015) Role of Pex21p for Piggyback Import of Gpd1p and Pnc1p into Peroxisomes of *Saccharomyces cerevisiae*. *J. Biol. Chem.* **290**, 25333–25342.

20. van Dijken JP, Otto R & Harder W (1976) Growth of *Hansenula polymorpha* in a methanol-limited chemostat. Physiological responses due to the involvement of methanol oxidase as a key enzyme in methanol metabolism. *Arch. Microbiol.* **111**, 137–144.
21. Huh W-K, Falvo JV, Gerke LC, Carroll AS, Howson RW, Weissman JS & O'Shea EK (2003) Global analysis of protein localization in budding yeast. *Nature* **425**, 686–691.
22. Güldener U, Heck S, Fiedler T, Beinhauer J & Hegemann JH (1996) A New Efficient Gene Disruption Cassette for Repeated Use in Budding Yeast. *Nucleic Acids Res.* **24**, 2519–2524.
23. Goldstein AL & McCusker JH (1999) Three new dominant drug resistance cassettes for gene disruption in *Saccharomyces cerevisiae*. *Yeast* **15**, 1541–1553.
24. Saraya R, Cepińska MN, Kiel JAKW, Veenhuis M & van der Klei IJ (2010) A conserved function for Inp2 in peroxisome inheritance. *Biochim. Biophys. Acta BBA - Mol. Cell Res.* **1803**, 617–622.
25. Kuravi K, Nagotu S, Krikken AM, Sjollem K, Deckers M, Erdmann R, Veenhuis M & van der Klei IJ (2006) Dynamin-related proteins Vps1p and Dnm1p control peroxisome abundance in *Saccharomyces cerevisiae*. *J. Cell Sci.* **119**, 3994–4001.
26. Krikken AM, Veenhuis M & van der Klei IJ (2009) *Hansenula polymorpha* pex11 cells are affected in peroxisome retention. *FEBS J.* **276**, 1429–1439.
27. Saraya R, Krikken AM, Kiel JAKW, Baerends RJS, Veenhuis M & van der Klei IJ (2012) Novel genetic tools for *Hansenula polymorpha*. *FEMS Yeast Res.* **12**, 271–278.
28. Shaner NC, Campbell RE, Steinbach PA, Giepmans BNG, Palmer AE & Tsien RY (2004) Improved monomeric red, orange and yellow fluorescent proteins derived from *Discosoma* sp. red fluorescent protein. *Nat. Biotechnol.* **22**, 1567–1572.
29. Leao-Helder AN, Krikken AM, van der Klei IJ, Kiel JAKW & Veenhuis M (2003) Transcriptional down-regulation of peroxisome numbers affects selective peroxisome degradation in *Hansenula polymorpha*. *J. Biol. Chem.* **278**, 40749–40756.
30. Lefevre SD, van Roermund CW, Wanders RJA, Veenhuis M & van der Klei IJ (2013) The significance of peroxisome function in chronological aging of *Saccharomyces cerevisiae*. *Aging Cell* **12**, 784–793.
31. Knoop K, Manivannan S, Cepińska MN, Krikken AM, Kram AM, Veenhuis M & van der Klei IJ (2014) Preperoxisomal vesicles can form in the absence of Pex3. *J. Cell Biol.* **204**, 659–668.

Supplementary data

Table S1. Yeast strains used in this study:-

Strains	Description	Reference
GPD1-GFP	WT, BY4741 MATa <i>leu2Δ0 met15Δ0 ura3Δ0</i> GFP is fused to endogenous Gpd1. <i>GPD1-GFP</i> is under control of the endogenous promoter	[21]
PNC1-GFP	WT, BY4741 MATa <i>leu2Δ0 met15Δ0 ura3Δ0</i> GFP is fused to endogenous Pnc1, resulting in <i>PNC1-GFP</i> under control of endogenous promoter	[21]
<i>GPD1-GFP</i> . DsRed-SKL	Gpd1-GFP containing plasmid encoding DsRed-SKL (pSL33/nat ^R)	This Study
<i>PNC1-GFP</i> . DsRed-SKL	Pnc1-GFP containing plasmid encoding DsRed-SKL (pSL33/nat ^R)	This study
<i>Δgpd1.PNC1-GFP</i>	BY4741 MATa <i>leu2Δ0 ura3Δ0</i> . <i>GPD1::KanMX4</i> . GFP is fused to endogenous Pnc1 resulting in <i>PNC1-GFP</i> under control of endogenous promoter	This study
<i>Δpnc1.GPD1-GFP</i>	BY4741 MATa <i>leu2Δ0 ura3Δ0</i> . <i>PNC1::KanMX4</i> producing <i>GPD1-GFP</i> under control of endogenous promoter	This study
<i>Δgpd1.PNC1-GFP</i> .DsRed-SKL	<i>Δgpd1</i> .Pnc1-GFP containing plasmid encoding DsRed-SKL (pSL33/nat ^R)	This study
<i>Δpnc1.GPD1-GFP</i> .DsRed-SKL	<i>Δpnc1</i> .Gpd1-GFP containing plasmid encoding DsRed-SKL (pSL33/nat ^R)	This study
<i>Δgpd1</i>	<i>GPD1::KanMX4</i> BY4742, MATa <i>his3A1 leu2A0 lys2A0 ura3A0</i>	Euroscarf
nΔgpd1	BY4742, <i>GPD1::KanMX4</i> pAG25-N_del_Gpd1	This study
nΔgpd1.PNC1-SKL	BY4742, <i>GPD1::KanMX4</i> pAG25-N_del_Gpd1, PTS1 (-SKL) is fused to endogenous Pnc1	This study
<i>ΔGPD1-mCherry</i> . GFP-SKL	BY4742, <i>GPD1::KanMX4</i> pAG25-N_del_Gpd1, mCherry introduced at the C-terminus of NΔGpd1 nat ^R zeo ^R pP _{TDH3} -GFP-SKL	This study
<i>PNC1-GFP.ΔGPD1-mCherry</i>	<i>Δgpd1</i> .Pnc1-GFP containing pAG25-N_del_Gpd1 mCherry introduced at the C-terminus of NΔGpd1 nat ^R zeo ^R	This study
<i>ΔGPD1-mCherry.Pnc1-SKL</i> . GFP-SKL	BY4742, pAG25-N_del_Gpd1/nat ^R zeo ^R <i>HghMX4</i> PTS1 (-SKL) is fused to endogenous Pnc1, pP _{TDH3} -GFP-SKL	This study
L-40	MATa <i>leu2 his3 trp1ade2 GAL4 gal80 LYS2::(lexAop)4-HIS3 URA3::(lexAop)s-lacZ</i>	Takara Bio Inc.
<i>POT1-GFP</i> . DsRed-SKL	Pot1-GFP under <i>GPD1</i> promoter, P _{GPD1} -Pot1-GFP, pSL33 nat ^R zeo ^R	This study

Table S2. Plasmids used in this study:-

Plasmids	Description	Reference
pUG6	loxP-KanMX4-loxP	[22]
pSL33	Gene encoding DsRed-SKL under control of <i>MET25</i> promoter, <i>nat</i> ^R	This study
pAG25	<i>nat</i> ^R , <i>amp</i> ^R , integrative	[23]
pAG25-N _{del} _Gpd1	pAG25 containing <i>NAGPD1</i> under control of <i>GPD1</i> promoter, <i>nat</i> ^R <i>amp</i> ^R	This study
pHIPZ4-mcherry	pRSA01, pHIPZ4-mCherry fusionator, <i>zeo</i> ^R <i>amp</i> ^R	This study
pPNC1-SKL-1	<i>PNC1-SKL</i> under control of <i>PNC1</i> promoter, <i>zeo</i> ^R <i>amp</i> ^R	This study
pBTM116-C	Yeast two-hybrid vector containing LexA binding domain, <i>amp</i> ^R , <i>TRP1</i>	Takara Bio Inc.
pVP16-C	Yeast two-hybrid vector containing LexA activation domain, <i>amp</i> ^R , <i>LEU2</i>	Takara Bio Inc.
pBTM116-PNC1	pBTM116-C containing <i>PNC1</i> coding region	This study
pVP16-PNC1	pVP16 containing <i>PNC1</i> coding region	This study
pBTM116- GPD1	pBTM116-C containing <i>GPD1</i> coding region	This study
pVP16-GPD1	pVP16 containing <i>GPD1</i> coding region	This study
pBTM116-PEX3	pBTM116-C containing <i>H. polymorpha</i> <i>PEX3</i> coding region	[24]
pVP16-PEX3	pVP16-C containing <i>H. polymorpha</i> <i>PEX3</i> coding region	[24]
pBTM116-PEX19	pBTM116-C containing <i>H. polymorpha</i> <i>PEX19</i> coding region	[24]
pVP16-PEX19	pVP16-C containing <i>H. polymorpha</i> <i>PEX19</i> coding region	[24]
pP _{TDH3} -GFP-SKL	<i>GFP-SKL</i> under control of <i>TDH3</i> promoter, <i>LEU2</i> <i>amp</i> ^R	This study
pP _{GPD1} -Pot1-GFP.	<i>POT1-GFP</i> under control of <i>GPD1</i> promoter, <i>zeo</i> ^R <i>amp</i> ^R	This study
pARM001	pHIPH4 containing <i>H. polymorpha</i> <i>PEX14</i> fused with mCherry hygromycine B ^R , <i>amp</i> ^R	This study
pSL34	<i>GFP-SKL</i> under control of <i>MET25</i> promoter <i>zeo</i> ^R <i>amp</i> ^R	[30]
pHIPN-PEX14- mCherry	Plasmid containing <i>H. polymorpha</i> <i>PEX14</i> fused to mCherry; <i>nat</i> ^R ; <i>amp</i> ^R	[31]
pHIPZ-mGFP fusinator	pHIPZ plasmid containing mGFP and <i>AMO</i> terminator; <i>zeo</i> ^R ; <i>amp</i> ^R	[24]
pBSII KS+	<i>amp</i> ^R , pUG6 origin of replication	Stratagene
pSL32	pBSII KS+ containing DsRed-SKL	This study
pHIPX7-GFP-SKL	Plasmid containing <i>GFP-SKL</i> ; <i>kan</i> ^R , <i>Sc-Leu2</i>	[26]
pHIPN-PEX14- mCherry	Plasmid containing <i>H. polymorpha</i> <i>PEX14</i> fused to mCherry; <i>nat</i> ^R ; <i>amp</i> ^R	[31]
pHIPH4	Plasmid containing <i>Klebsiella pneumoniae</i> Hygromycin B ^R Amp ^R	[27]
pCDNA3.1mCherry	Plasmid containing mCherry, <i>amp</i> ^R	[28]
pANL31	pHIPZ-eGFP fusionator, <i>amp</i> ^R	[20]
pUG34-DsRed-SKL	<i>DsRed-SKL</i> under control of <i>MET25</i> promoter, CEN, <i>HIS3</i>	[27]

Table S3. Primers used in this study

Primers	Sequence
GPD1F	TATATGTACACCCCCCCCCTCCACAAACACAAATATTGATAATATAAA GCAGCTGAAGCTTCGTACGC
GPD1R	CCTCGAAAAAAGTGGGGGAAAGTATGATATGTTATCTTTCTCCAATAA ATGCATAGGCCACTAGTGGATCTG
PNC1F	TTTTACGATTATCTATATCTTTGTTAGAAAGAATAAAATACAGTACAAA ACAGCTGAAGCTTCGTACGC
PNC1R	CATTTGCAAGCCACCCTAGTTCATCAGGTTGAAGAAGTATTATTCAGC TCGCATAGGCCACTAGTGGATCTG
GPD1.OL-1	CACAAATATTGATAATATAAAGATGGGTAGAAAGAGAAGTTCCTC
GPD1.OL-1.1	CATGGATCCGACAGCCTCTGAATGAGT
GPD1.OL-2	GAGGAACTTCTCTTTCTACCCATCTTTATATTATCAATATTTGTG
GPD1.OL-2.1	CACAAGCTTCTCGGTAGATCAGGTCAGTA
GPD1.MC_F	CAATGAAGAACCTGCCGGACATGATTGAAGAATTAGATCTACATGAAG ATGTGAGCAAGGGCGAGGAGG
GPD1.MC_R2	CCTCGAAAAAAGTGGGGGAAAGTATGATATGTTATCTTTCTCCAATAA ATAACGACGGCCAGTGAATTGT
P.SKL.F_BamHI	TTATATGGATCCGCGAGGCTGCAGTCACC
P.SKL.R_HindIII	CGGCGCAAGCTTCTAGAGTTTGTAGTGCAGTGGTTGTATAGTTTATC CACGACATTGATGT
PNC1.7	CCTTCCACGACATCTGGAAC
PNC1.GFP.SKL-2.2	CATTTGCAAGCCACCCTAGTTCATCAGGTTGAAGAAGTATTATTCAGC TCGTTGGCCGATTTCATTAAT
GPD1.MC_Rev	CCTCGAAAAAAGTGGGGGAAAGTATGATATGTTATCTTTCTCCAATAA ATCCATGATTACGCCAAGCTC
PNC1.BamHI.F	CGCGGATCCATGAAGACTTTAATTGTTGTTGATAT
PNC1.EcoRI.R	CCGGAATTCTTATTTATCCACGACATTGATGT
GPD1.BamHI.F	CGCGGATCCATGTCTGCTGCTGCTGATAGA
GPD1.EcoRI.F	CCGGAATTCTTAATCTTCATGTAGATCTAATTCCTC
TDH3_NotI.F	GCATCAGCGGCCGCCACGCTTTTTCAGTTCGAGT
TDH3_BamHI.R	GCGCGCGGATCCTTTGTTGTTTATGTGTGTTTAT
PRARM001 FWD	ATAGCGGCCGCTTGCAGGAAAGTCGACGAAAT
PRARM002 REV	CGGAAGCTTTTACTTGTACAGCTCGTCCA
NAT1.1	GGCTCTAGACGTTAGAACGCGGCTACAAT
NAT1.2	TCTCCGCGGGCTCGTTTTCGACACTGGAT
DsRed-1	CACGGTACCTAACGCCAGGGTTTTC
DsRed-2	CGCTCTAGACGCGCAATTAACCCTC
P-GPD1.PciI	GCACTACATGTTCCCTCCACAAAGGCCTCTC
GPD1.OL-Rev	CTTTGTAGTCTTTGAGACATCTTTATATTATCAATATTTGTG
POT1.OL-Fw	CACAAATATTGATAATATAAAG ATGTCTCAAAGACTACAAAG
POT1-BglII	GAGCGAGATCTTTCTTTAATAAAGATGGCGG
RSA10fw	GAAGATCTATGGTGAGCAAGGGCGAGGAG
RSA11rev	GCGTGTCGACTTACTTGTACAGCTCGTCCATGCC

